AIAA JOURNAL
Vol. 31, No. 11, November 1993

Improved Control Design Variable Linking for Optimization of Structural/Control Systems

Ik Min Jin* and Lucien A. Schmit†
University of California, Los Angeles, Los Angeles, California 90024

A method is presented to integrate the design space for structural/control system optimization problems in the case of linear state feedback control. To make the truly simultaneous optimization of structural/control systems tractable, without increasing the number of control design variables, the conventional structural design variable linking idea is extended to the control system feedback gain matrix. In this paper a new control design variable linking scheme based on representing the feedback gain matrix as the linear combination of component matrices corresponding to different modes is introduced. The original nonlinear mathematical programming problem based on a finite element formulation and linear state feedback is replaced by a sequence of explicit approximate problems exploiting various approximation concepts such as structural and control design variable linkings, temporary constraint deletion, and first-order Taylor series expansion of nonlinear behavior constraints in terms of intermediate design variables. Examples that involve a variety of dynamic behavior constraints (including constraints on closed-loop eigenvalues, peak transient displacements, and peak actuator forces) are effectively solved by using the improved control design variable linking scheme presented.

I. Introduction

LARGE space structures usually have low stiffness and low damping characteristics due to their light weight requirements. To suppress the vibration and maintain the strict shape specifications, it is necessary to enhance stiffness and/or damping of the structures through some type of active controls.[1] In Refs. 2 and 3 it has been shown that slight structural modification can lead to a considerable improvement in the control system performance, and there has been a considerable effort to integrate the design optimization of structures and control systems to achieve a better performance and directly handle cross coupling effects and dynamic interactions between the two systems.

Most of this research has focused on linear control laws based on output feedback or state feedback. In the case of output feedback, several studies have been made in which the structural dimensions and the control gains are treated as strictly independent design variables in optimization.[4-7] On the other hand, in the case of full state feedback control, a sequential approach is usually adopted in which the control gains are determined by solving Riccati equations corresponding to the changing structural system during design iterations.[8-11] When the gain variables are determined by solving Riccati equations for a fixed plant, they implicitly become dependent design variables and the resulting design optimization is constrained to a subspace where the optimality conditions of a control subproblem are satisfied. The tendency to subordinate gains to a dependent variable status can be attributed to the fact that for system models with a large number of degrees of freedom, the feedback gain matrix $[H]$ contains prohibitively large numbers of independent design variables (i.e., $M \times 2N$ control design variables, where M is the number of actuators and N is the number of degrees of freedom in the system model).

In Ref. 12, both the structural cross-sectional dimensions (CSDs) and control gains were treated as strictly independent design variables in the case of linear state feedback control. True design space integration was achieved using relatively small numbers of independent control system design variables by introducing several control design variable linking schemes based primarily on column-wise and row-wise linking in the gain matrix. In the current paper, alternative block-type control variable linking schemes are introduced.

II. Problem Statements

The simultaneous structural/control optimization problem is formulated as a general nonlinear inequality constrained mathematical programming problem as follows:

Find Y to minimize $F(Y)$ subject to

$$G_j(Y) \leq 0, \qquad j = 1, \ldots, NCON \tag{1}$$

with bounds

$$Y_i^L \leq Y_i \leq Y_i^U, \qquad i = 1, \ldots, \mathrm{NDV}$$

where NDV is the total number of design variables, $Y = \lfloor Y_1, Y_2, \ldots, Y_{\mathrm{NDV}} \rfloor^T$ is an NDV $\times$ 1 design variable vector, F is a scalar objective function, G_j is the jth behavior constraint, $NCON$ is the total number of behavior constraints, and Y_i^L and Y_i^U are side constraints on the ith design variable, respectively.

Both structural and control design variables are included independently in the design variable vector Y. The total mass of the system has been chosen as the objective function, and constraints on 1) dynamic stability (real parts of closed-loop eigenvalues), 2) damped frequencies (imaginary parts of closed-loop eigenvalues), 3) peak transient responses, and 4) peak transient control forces are included in this study.

III. Structural/Control System Description

The second-order equations of motion are

$$[M]\{\ddot{q}\} + [C]\{\dot{q}\} + [K]\{q\} = [b]\{u\} + [e]\{f\} \tag{2}$$

where $\{q\}$ is an $N \times 1$ vector of nodal degrees of freedom (DOF); $\{\dot{q}\}$ and $\{\ddot{q}\}$ are first and second time derivatives of $\{q\}$; $[M]$, $[K]$, and $[C]$ are $N \times N$ mass, stiffness, and damping matrices, respectively; $\{u\}$ is an $M \times 1$ actuator force

Presented as Paper 92-1241 at the AIAA Aerospace Design Conference, Irvine, CA, Feb. 3–6, 1992; received May 19, 1992; revision received Nov. 6, 1992; accepted for publication Dec. 2, 1992.

*Postdoctoral Research Associate, Mechanical, Aerospace and Nuclear Engineering Department; currently Senior Researcher, Korean Aerospace Research Institute. Member AIAA.

†Rockwell Professor of Aerospace Engineering, Emeritus, 5532 Boelter Hall. Fellow AIAA.

vector; M is the number of actuators; $\{f\}$ is an $L \times 1$ vector of external disturbances; L is the number of external disturbances making up a single load condition; and $[b]$ and $[e]$ are $N \times M$ and $N \times L$ coefficient matrices consisting of the directional cosines, which relate actuator and disturbance forces to the nodal DOFs, respectively.

It is assumed that the preassigned damping inherent to the structure can be represented by a proportional damping matrix, which is a linear combination of the structural mass and stiffness matrices, i.e.,

$$[C] = c_M[M] + c_K[K], \qquad c_M, c_K \text{ constants} \tag{3}$$

Equation (2) can be transformed into the first-order state space equation as follows:

$$\{\dot{x}\} = [A_o]\{x\} + [B]\{u\} + [E]\{f\} \tag{4}$$

where

$$\{x\}^T = \lfloor \{q\}^T \{\dot{q}\}^T \rfloor$$

$$[A_o] = \begin{bmatrix} [0] & [I] \\ -[M]^{-1}[K] & -[M]^{-1}[C] \end{bmatrix}$$

$$[B] = \begin{bmatrix} [0] \\ [M]^{-1}[b] \end{bmatrix} \qquad [E] = \begin{bmatrix} [0] \\ [M]^{-1}[e] \end{bmatrix}$$

The control input vector $\{u\}$ is to be determined under the assumption that all of the states (components of $\{x\}$) are available, that is

$$\{u\} = -[H]\{x\} = -\begin{bmatrix} [H_p] & [H_v] \end{bmatrix} \begin{Bmatrix} q \\ \dot{q} \end{Bmatrix} \tag{5}$$

where $[H]$ is the $M \times 2N$ feedback gain matrix and $[H_p]$ and $[H_v]$ are the $M \times N$ position and velocity parts of $[H]$, respectively. The closed-loop state equation becomes

$$\{\dot{x}\} = [A]\{x\} + [E]\{f\} \tag{6}$$

where the closed-loop system matrix $[A]$ is

$$[A] = [A_o] - [B][H]$$

IV. Generation of Basis Matrices for Improved Control Design Variable Linking

Initial control gains are obtained by solving a set of 2×2 Riccati equations corresponding to the initial structure (see Ref. 12). The solution procedure is reviewed in the following paragraphs.

First find the natural frequencies and normal modes of

$$[M]\{\ddot{q}\} + [K]\{q\} = \{0\} \tag{7}$$

that is, solve the standard eigenproblem

$$\omega_i^2[M]\{v_i\} = [K]\{v_i\}, \qquad i = 1, 2, \ldots, r \tag{8}$$

and normalize the modes $\{v_i\}$ so that

$$\{v_i\}^T[M]\{v_j\} = \delta_{ij}, \qquad i, j = 1, 2, \ldots, r \tag{9}$$

where δ_{ij} is the Kronecker data, and r is the number of normal modes to be used in the decoupled Ricatti equation solution ($r \le N$). Note that r should be at least equal to or greater than the number of structural modes to be controlled. Let

$$\{q\} = [V]\{z\} \tag{10}$$

where the ith column of the $N \times r$ normal mode matrix $[V]$ is the ith normal mode $\{v_i\}$ and $\{z\} = \lfloor z_1, z_2, \ldots, z_r \rfloor^T$ is an $r \times 1$ normal coordinate vector. Substituting Eq. (10) into Eq. (2) (assuming $\{f\} = \{0\}$) and premultiplying by $[V]^T$ results in r sets of scalar equations as follows:

$$\ddot{z}_i + c_i\dot{z}_i + \omega_i^2 z_i = \{v_i\}^T[b]\{u\}$$
$$= \{v_i\}^T[b]\left(\{u\}^{(i)} + \sum_{k \ne 1}^{r} \{u\}^{(k)}\right) \tag{11}$$

where

$$\{u\}^{(i)} = -\{[\tilde{H}_p]^{(i)}[\tilde{H}_v]^{(i)}\}\begin{Bmatrix} z_i \\ \dot{z}_i \end{Bmatrix}, \qquad i = 1, 2, \ldots, r \tag{12}$$

The vector $\{u\}^{(i)}$ is an $M \times 1$ control vector that contains only the ith normal mode components (z_i and $\dot{z}_i$). Furthermore, $\{\tilde{H}_p\}^{(i)}$ and $\{\tilde{H}_v\}^{(i)}$ are $M \times 1$ feedback gain vectors which relate $\{u\}^{(i)}$ with z_i and $\dot{z}_i$, respectively. It is noted that $c_i = c_M + c_K\omega_i^2$, in view of the proportional damping assumption embodied in Eq. (3).

Equation (11) can be rewritten as

$$\ddot{z}_i + c_i\dot{z}_i + \omega_i^2 z_i = \{v_i\}^T[b]\{u\}^{(i)} + \{f\}^{(i)} \tag{13}$$

where

$$\{f\}^{(i)} = \{v_i\}^T[b]\sum_{k \ne i}^{r}\{u\}^{(k)}$$

Note that the coupling terms $\{f\}^{(i)}$ contain modal components other than the ith mode and can be treated as disturbance forces for the ith modal equation. To determine the optimal control $\{u\}^{(i)}$, Eq. (13) can be transformed into the standard first-order state space form neglecting the coupling terms as follows:

$$\{\dot{w}_i\} = [A_i]\{w_i\} + [B_i]\{u\}^{(i)}$$
$$[A_i] = \begin{bmatrix} 0 & 1 \\ -\omega_i^2 & -c_i \end{bmatrix}, \qquad [B_i] = \begin{bmatrix} [0] \\ \{v_i\}^T[b] \end{bmatrix} \tag{14}$$

where $\{w_i\} = \lfloor z_i \ \dot{z}_i \rfloor^T$ is the 2×1 state vector, $[A_i]$ is the 2×2 system open-loop matrix, and $[B_i]$ is the $2 \times M$ system input matrix for the ith modal equation.

The performance index for the ith mode (PI_i) is chosen as

$$PI_i = \int_0^\infty \left(\{w_i\}^T[Q_i]\{w_i\} + \{u\}^{(i)T}[R_i]\{u\}^{(i)}\right) dt \tag{15}$$

where $[Q_i] = \text{diag}[Q_{11}^i, Q_{22}^i]$ ($Q_{11}^i, Q_{22}^i \ge 0$) is a 2×2 diagonal weighting matrix for the ith state vector and $[R_i] = \gamma_i[I]$ ($[I]$ is an $M \times M$ identity matrix, $\gamma_i > 0$) is a weighting matrix for the ith modal control force vector. Then the ith control force vector $\{u\}^{(i)}$ can be determined from

$$\{u\}^{(i)} = -[R_i]^{-1}[B_i]^T[P_i]\{w_i\}^{(i)}$$
$$= -\frac{1}{\gamma_i}[b]^T\{v_i\}p_{12}^i z_i - \frac{1}{\gamma_i}[b]^T\{v_i\}p_{22}^i\dot{z}_i \tag{16}$$

where the 2×2 positive semidefinite symmetric matrix

$$[P_i] = \begin{bmatrix} p_{11}^i & p_{12}^i \\ p_{12}^i & p_{22}^i \end{bmatrix}$$

satisfies the 2×2 Riccati equation

$$[P_i][A_i] + [A_i]^T[P_i] + [Q_i] - [P_i][B_i][R_i]^{-1}[B_i]^T[P_i] = [0] \tag{17}$$

which can be solved in closed form (see Appendix B of Ref. 13). By comparing Eq. (12) and Eq. (16), the ith feedback gain vectors in normal coordinates can be obtained as follows:

$$\{\tilde{H}_p\}^{(i)} = \frac{p_{12}^i}{\gamma_i}[b]^T\{v_i\}, \qquad \{\tilde{H}_v\}^{(i)} = \frac{p_{22}^i}{\gamma_i}[b]^T\{v_i\} \quad (18)$$

Now assume that the control vector $\{u\}$ is the sum of the various $\{u\}^{(i)}$, each of which is calculated independently neglecting the coupling term [second term on the right-hand side of Eq. (11)], i.e.,

$$\{u\} \cong \sum_{i=1}^{r}\{u\}^{(i)} = -\left[[\tilde{H}_p]\;[\tilde{H}_v]\right]\begin{Bmatrix} z \\ \dot{z}\end{Bmatrix} \quad (19)$$

where $[\tilde{H}_p]$ and $[\tilde{H}_v]$ denote $M \times r$ position and velocity gain matrices in normal coordinates, the columns of which are $\{\tilde{H}_p\}^{(i)}$ and $\{\tilde{H}_v\}^{(i)}$, respectively. Then using the relation $\{z\} = [V]^T[M]\{q\}$ [premultiply Eq. (10) by $[V]^T[M]$ and note that $[V]^T[M][V] = [I]$ in view of Eq. (9)], the initial feedback gain matrix in physical coordinates $[H^o]$ can be recovered as follows:

$$[H^o] = \left[[H_p^o]\;[H_v^o]\right] \quad (20)$$

$$[H_p^o] = [\tilde{H}_p][V]^T[M] \quad (21)$$

$$[H_v^o] = [\tilde{H}_v][V]^T[M] \quad (22)$$

where superscripts o denote initial feedback gain matrices.

In Ref. 12 several linking schemes for the feedback gain matrix were introduced. They were based on 1) separation of velocity and position parts of the gain matrix, 2) various row and column schemes corresponding to actuator and degree of freedom linking, and 3) linking schemes based on only allowing changes in various sets of velocity gains. Combining the foregoing ideas led to numerous linking schemes with distinct sets and various numbers of independent control system design variables (CDV), ranging from 1 to $M \times 2N$ (see Table 1 of Ref. 12).

In this paper a new approach to linking of control design variables is introduced and assessed. The initial feedback gain matrix obtained by solving r sets of 2×2 Riccati equations [Eqs. (20–22)] can be rewritten in the following form:

$$[H^o] = \left[[H_p^o]\;[H_v^o]\right] = \sum_{i=1}^{r}\left[[H_p^o]^{(i)}\;[H_v^o]^{(i)}\right] = \sum_{i=1}^{r}[H^o]^{(i)} \quad (23)$$

$$[H_p^o] = \sum_{i=1}^{r}\{\tilde{H}_p\}^{(i)}\{v_i\}^T[M] = \sum_{i=1}^{r}[H_p^o]^{(i)} \quad (24)$$

$$[H_v^o] = \sum_{i=1}^{r}\{\tilde{H}_v\}^{(i)}\{v_i\}^T[M] = \sum_{i=1}^{r}[H_v^o]^{(i)} \quad (25)$$

where superscripts (i) indicate that these quantities correspond to the ith Riccati equation. The foregoing equations imply that the $[H_p^o]^{(i)}$ and $[H_v^o]^{(i)}$ or the $[H^o]^{(i)}$ may be interpreted as basis matrices, which can be used to generate the initial gain matrix. This use suggests that the actual feedback gain matrix can be well approximated as a linear combination of these basis matrices, namely

$$[H] = \sum_{i=1}^{r}\alpha_i[H^o]^{(i)} \quad (26)$$

or

$$[H] = \sum_{i=1}^{r}\left[\alpha_i[H_p^o]^{(i)}\quad \alpha_{i+r}[H_v^o]^{(i)}\right] \quad (27)$$

The whole feedback gain matrix can be linked [Eq. (26)], or the position and velocity parts of the gain matrix can be block linked separately [Eq. (27)]. During the optimization the participation coefficients α_i are treated as independent design variables along with the structural sizing variables. It should be noted that these participation coefficients can be further linked with each other. It is important to recognize that in this work the closed-form solution of the decoupled Riccati equations (see Appendix B, Ref. 13) is used exclusively for the purpose of generating basis matrices [Eqs. (26) and (27)].

V. Optimization

Various approximation concepts such as structural and control design variable linking, temporary constraint deletion, and intermediate design variables[14,15] are used to replace the original design optimization problem by a series of explicit approximate problems. Linear, reciprocal, or hybrid approximations (see Refs. 16 and 17) can be generated with respect to either direct or intermediate design variables, even though the approximate design optimization problems are always solved in an integrated design space that spans the independent structural CSDs and the participation coefficients of the linked control gains. Each approximate optimization problem has its own lower and upper bounds on the design variables. These bounds are determined by the move limits or the original side constraints [see Eq. (1)], whichever is most restrictive. For frame elements it is known that the section properties A, I_y, I_z, and J are a good choice for intermediate design variables. This knowledge follows from the fact that the elements of the stiffness and the mass matrices are linear functions of these section properties. Control design variables are used directly in the generation of the approximate problems because the system matrices are linear functions of the gains.

With the information acquired from the analysis and sensitivity analysis phase (see Ref. 13 for details) each approximate optimization problem can be formulated as follows:

Find Y to minimize $\tilde{F}[X(Y)]$ subject to

$$\tilde{G}_j[X(Y)] \le 0, \qquad j \in Q_R \quad (28)$$

with bounds

$$\underline{Y}_i \le Y_i \le \overline{Y}_i, \qquad i = 1, \ldots, \text{NDV}$$

where Y is a vector of design variables (NDV $\times$ 1), $X(Y)$ is a vector of intermediate design variables, $\tilde{F}(\cdot)$ is an approximate objective function, $\tilde{G}_j(\cdot)$ is the jth approximate constraint, $\underline{Y}_i$ and $\overline{Y}_i$ are lower and upper bounds for the ith design variable (during solution of the current optimization problem), and Q_R is the retained set of constraints for the current approximate problem. For all of the numerical examples presented in this paper, the following approximation options are employed. Linear approximation of $\tilde{F}(\cdot)$ is used with respect to intermediate structural design variables (A, I_y, I_z, J), which is exact when the mass is minimized. When generating the approximate constraint functions $\tilde{G}_j(\cdot)$, linear approximation is chosen with respect to control design variables, whereas the hybrid approximation is used with respect to structural intermediate design variables.

VI. Numerical Results

The control augmented structural optimization solution method described in the preceding sections has been implemented on the IBM 3090 mainframe computer at the University of California, Los Angeles. CONMIN[18] is used as the optimizer. Numerical results that illustrate effectiveness of various block-type control design variable linking schemes are presented here.

Example 1: Antenna Structure

An idealized antenna structure is chosen as the first example to be presented here. It consists of eight aluminum beams

($E = 7.3 \times 10^6$ N/cm^2, $\rho = 2.77 \times 10^{-3}$ kg/cm^3, $\nu = 0.325$) that have thin-walled hollow-box-beam cross sections (see Fig. 1). This structure is constrained to move vertically (Y direction) only, so each nodal point has 3 DOF (translation in the Y direction and rotation about the X and Z reference axes shown in Fig. 1) resulting in the total 18 DOF (N = 18). Nodal point coordinates and the corresponding degrees of freedom are given in Table 1. Four translational actuators ($M = 4$) weighing 4 kg each are attached to nodes 3, 5, 6, and 7. These actuators are oriented so that the force they generate acts in the vertical direction (degrees of freedom 4, 10, 13, and 16). Two ramp-type transient loads are applied to node 3 at the same time. One is a vertical force $[f_1(t)]$ and the other is a moment $[f_2(t)]$ about a line parallel to the X reference axis but passing through node 3, which gives antisymmetric exitation. These loads are given as follows:

$$f_1(t) = 333.3t \text{ N}, \qquad f_2(t) = 10.0 \times f_1(t) \text{ N} \cdot \text{cm}$$

for $0 \le t \le 0.3$ s, and $f_1(t) = f_2(t) = 0$ for $t > 0.3$ s (see Fig. 1). Transient response is considered for the time interval $0 \le t \le 2$ s, and 20 out of 36 complex modes are used to calculate the peak response values. Passive damping is assumed to be zero ($c_M = c_K = 0$). This assumption tends to be conservative for transient response constraints, and it is further justified by observing that the magnitude of damping inherent to the structural system is likely to be small compared with that introduced by an active control system.

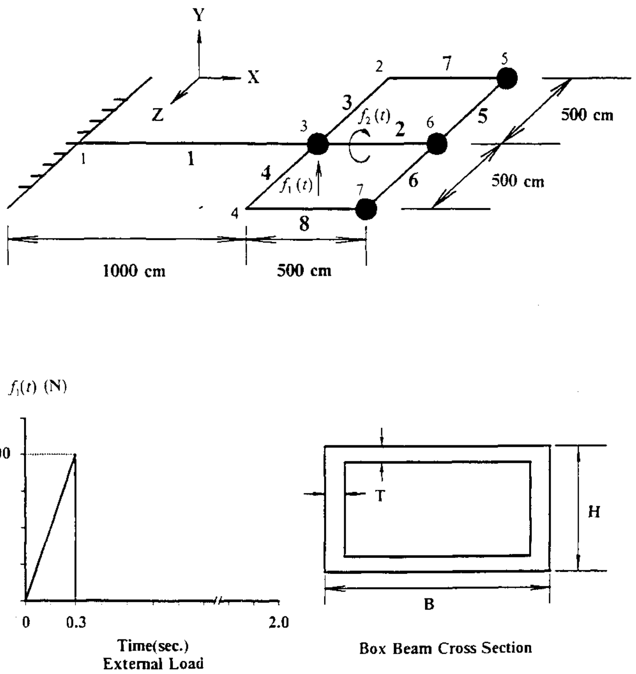

Fig. 1 Antenna structure.

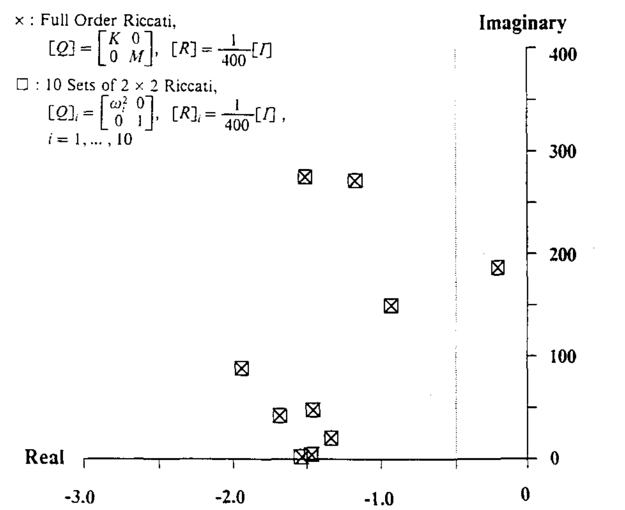

Fig. 2 Comparison of initial closed-loop eigenvalues, antenna structure.

Table 1 Nodal point data, antenna structure

Node no.	Coordinates, cm			Degrees of freedom		
	X	Y	Z	Y trans.	X rot.	Z rot.
1	0	0	0	—	—	—
2	1000	0	−500	1	2	3
3	1000	0	0	4	5	6
4	1000	0	500	7	8	9
5	1500	0	−500	10	11	12
6	1500	0	0	13	14	15
7	1500	0	500	16	17	18

The design objective to be minimized is the total mass of the system including the fixed actuator masses as well as the variable structural mass. Flange and web thicknesses are constrained to be the same, so that there are three structural design variables for each finite element (B, H, and T). Structural linking is also used to make the structure remain symmetric with respect to the XY plane, which results in the total 15 independent structural design variables. The initial structure is uniform ($B = H = 20.0$ cm, $T = 0.5$ cm), and the side constraints are $10.0 \text{ cm} \le B, H \le 25.0$ cm, and $0.1 \le T \le 1.0$ cm.

Move limits of 20 to 70% for both structural variables and control variables are used. The convergence criteria used in this example is that for two consecutive iterations the relative difference in the objective function should be less than 0.1%. In all cases behavior constraints are imposed on 1) the real part of all of the retained complex modes ($\sigma_i \le -0.5$); 2) the fourth and fifth damped frequencies ($\omega_{d_4} \ge 8.0$ Hz, $\omega_{d_5} \ge 9.25$ Hz); 3) the peak displacement of nodes 2, 4, 5, and 7 ($|q_i(t)| \le 1.0$ cm, $i = 1$, 7, 10, and 16); and 4) the peak actuator force ($|u_j(t)| \le 8.5$ N, $j = 1$, 2, 3, and 4). Initial startup gains are computed by solving 10 sets of 2×2 Riccati equations ($r = 10$). The 2×2 state weighting matrices are set to be $[Q_i] = \text{diag}[\omega_i^2, 1]$, $i = 1, 2, \ldots, r$, so that the first term of Eq. (15) represents a total (strain and kinetic) modal energy, and the control weighting coefficients γ_i are chosen to be 1/400. In Fig. 2, the initial closed-loop eigenvalues ($\lambda_i = \sigma_i + j\omega_{d_i}$) obtained by solving 10 sets of 2×2 Riccati equations are compared with those obtained from a full-order Riccati equation solution, and, as can be seen from the plot, these two solution methods give almost the same values for the lowest 10 modes.

At the initial design constraints on the real part of the eighth closed-loop eigenvalue, two of the damped frequencies are violated ($\sigma_8 = -0.025 > -0.5$, $\omega_{d_4} = 6.74 < 8.0$ Hz and $\omega_{d_5} = 7.61 < 9.25$ Hz). Furthermore, three of the peak control force constraints are initially violated $[|u_2(t)|_{max} = 8.76 > 8.5$ N, $|u_3(t)|_{max} = 9.26 > 8.5$ N, and $|u_4(t)|_{max} = 9.33 > 8.5$ N$]$, but all of the peak displacement constraints are satisfied.

Case 0, No Control Design Variable Linking

This case does not use any control design variable linking scheme, therefore, 15 structural cross-sectional dimensions and all 144 ($= M \times 2N$) elements of the feedback gain matrix are treated as independent design variables. Since this case has full design space freedom, the solution mass of this case is expected to be the lowest value for the entire example. The iteration history and the final structural design are given in Tables 2 and 3, respectively. At the final design all of the constraints are satisfied and the critical constraints are 1) the tenth real part of closed-loop eigenvalues (σ_{10}); 2) the fourth damped frequency (ω_{d_4}); 3) the peak displacements at nodes 5 and 7 (q_{10} and q_{16}); and 4) the peak control forces of all four actuators (u_1, u_2, u_3, and u_4).

Cases 1-10, Linking on [H]

Cases 1-10 select participation coefficients α_i of $[H^o]^{(i)}$ [see Eq. (26)] as design variables. These α_i are further linked so that in each case the number of independent control design variables is different. The basic scheme employed here is to treat the first $(K-1)$ variables $\alpha_1, \ldots, \alpha_{K-1}$ as independent and then link all of the remaining variables $\alpha_K = \alpha_{K+1} = \cdots = \alpha_{10}$ so that the total number of independent control design variables after linking is K. For example, when $K = 1$ there is only one independent design variable after linking, since $\alpha_1 = \alpha_2 = \cdots = \alpha_{10}$. When $K = 2$ there are two independent design variables after linking, namely α_1 and $\alpha_2 = \alpha_3 = \cdots = \alpha_{10}$. Finally, when $K = 10$ there will be 10 independent design variables after linking, namely the participation coefficients of the 10 basis matrices in Eq. (26).

Iteration histories and final structural designs for cases 1-10 are given in Tables 4 and 5. In Fig. 3, iteration histories of some cases are graphically compared with each other and with case 0, which serves as the reference solution.

Table 2 Iteration history, antenna structure, case 0

Analysis	Total mass, kg
1	502.14
2	462.20
3	345.34
4	254.17
5	213.91
6	184.11
7	174.34
8	168.93
9	169.35
10	165.61
11	164.42
12	164.08
13	164.17
14	163.99
15	163.76
16	163.20
17	163.10
18	163.11

Table 3 Final structural design, antenna structure, case 0 (cross-sectional dimensions, cm)

	Element 1	Element 2	Elements 3, 4	Elements 5, 6	Elements 7, 8
B	25.00[a]	25.00[a]	23.24	25.00[a]	19.31
H	25.00[a]	25.00[a]	25.00[a]	25.00[a]	25.00[a]
T	0.1000[b]	0.1108	0.1000[b]	0.1935	0.1000[b]

[a]Indicates upper bound value. [b]Indicates lower bound value.

Cases 11-20, Linking on $[H_p]$ and $[H_v]$

Cases 11-20 are the same as cases 1-10 except that position and velocity parts of the gain matrix are separated. Namely, the α_i of both $[H_p^o]^{(i)}$ and $[H_v^o]^{(i)}$ [see Eq. (27)] are candidates for design variables, so that the maximum number of independent control design variables after linking is doubled from 10 to 20. Iteration histories and final structural designs are given in Tables 6 and 7 and Fig. 4.

Summary and Discussion

As the freedom in the design space is increased by choosing more independent control design variables (from case 1 to case 10 and from case 11 to case 20), it can be clearly seen from the results that the optimum mass decreases. Table 8 shows critical constraints $(-0.03 \leq G_j \leq 0.0004)$ at the final designs. Fourth damped frequency (ω_{d_4}), peak displacement at node 7 (q_{16}), and peak control force at node 7 (u_4) are critical in all cases.

It is important to note that even with only one or two independent control design variables (cases 1 and 11), the final mass values obtained (206.06 and 204.16 kg) are about 15% lower than the result reported in Ref. 8 (241.97 kg). This result can be attributed to the fact that in Ref. 8 the control gains are not independent design variables since, for any particular set of structural design variables, they are determined from the solution of a linear quadratic regulator subproblem.

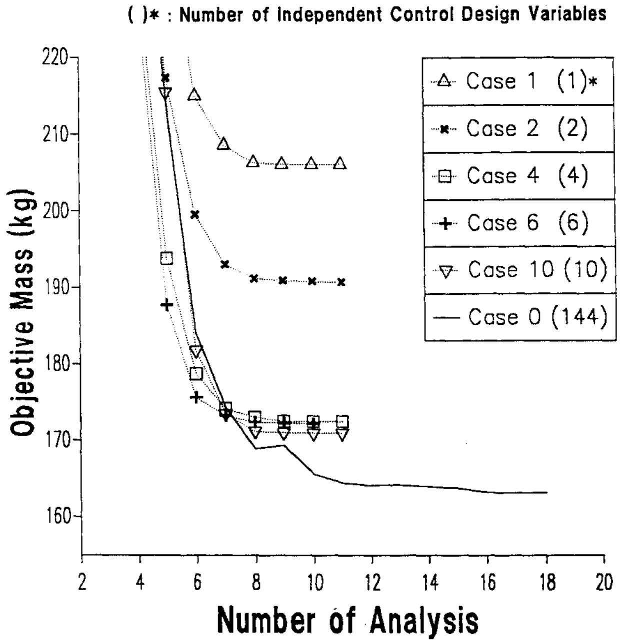

Fig. 3 Antenna structure iteration histories, cases 1-10.

Table 4 Iteration histories, antenna structure, cases 1-10 (total mass, kg)

Analysis	Case 1 (1[a])	Case 2 (2[a])	Case 3 (3[a])	Case 4 (4[a])	Case 5 (5[a])	Case 6 (6[a])	Case 7 (7[a])	Case 8 (8[a])	Case 9 (9[a])	Case 10 (10[a])
1	502.14	502.14	502.14	502.14	502.14	502.14	502.14	502.14	502.14	502.14
2	484.61	470.88	471.87	444.12	454.83	453.14	449.81	450.11	435.15	469.10
3	387.64	328.11	328.47	303.50	346.62	299.54	293.56	294.62	307.14	350.45
4	297.69	260.67	254.76	233.56	268.66	228.72	217.54	218.41	228.31	268.09
5	240.14	217.39	214.99	193.83	215.70	187.80	184.73	180.21	188.59	215.51
6	215.05	199.59	200.57	178.76	185.24	175.65	176.29	174.64	175.95	181.14
7	208.60	193.04	192.60	174.18	175.46	173.27	173.07	174.70	173.41	173.50
8	206.33	191.20	190.47	173.05	176.56	172.41	172.28	174.38	172.68	171.19
9	206.07	190.90	190.23	172.50	173.25	172.29	171.93	173.93	171.10	171.02
10	206.06	190.80	190.14	172.46	172.66	172.17	171.80	171.27	170.84	170.96
11	206.06	190.70	189.94	172.46	172.46		171.73	170.97	170.70	170.92
12			189.85		172.37			170.84	170.65	
13			189.91		172.32			170.81		

[a]Number of independent control design variables.

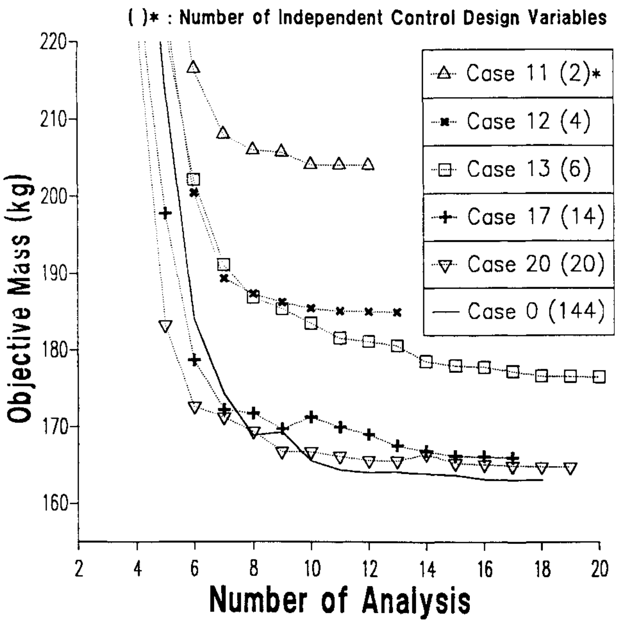

Fig. 4 Antenna structure iteration histories, cases 11–20.

In Fig. 5 final masses are compared with the number of independent control variables. Compared with the results reported in Ref. 12, based on the column-wise or row-wise linking schemes, the new block-type (basis matrix) linking method introduced here gives much better results in the sense that with the same or fewer independent control design variables significantly lower final design mass can be obtained.

Example 2: Grillage Structure

The second example is the 4×6 planar grillage structure (see Fig. 6) that was studied in Refs. 5 and 8. It consists of a lattice of 10 aluminum frame members placed on 2-ft centers and cantilevered from two fixed supports by 2-ft-long flexible beams ($E = 10.5 \times 10^6$ psi, $\rho = 0.1$ lb/in.^{3}, $\nu = 0.3$). Each solid rectangular member is 2.0 in. wide (fixed) and has an initial depth (variable) of 0.25 in. The members are oriented so that the width dimensions lie in the plane of the structure (*XZ* plane). The grillage is modeled using 40 finite elements, each of which is 2 ft long, and the total number of DOF is 72 (3 per node at 24 nodes). A small amount of passive damping [$c_M = 0$, $c_K = 0.00005$, see Eq. (3)], which gives passive damping ratios between 0.0059% (1st mode) and 0.36% (20th mode) to the uncontrolled initial structure, is assumed to exist. Four torque actuators are placed to provide control torque in

Table 5 Final structural designs, antenna structure, cases 1–10 (cross-sectional dimensions, cm)

	Case	Element 1	Element 2	Elements 3, 4	Elements 5, 6	Elements 7, 8	Case	Element 1	Element 2	Elements 3, 4	Elements 5, 6	Elements 7, 8
B		25.00[a]	25.00[a]	19.62	25.00[a]	15.51		25.00[a]	25.00[a]	18.72	25.00[a]	21.03
H	1	25.00[a]	25.00[a]	25.00[a]	25.00[a]	25.00[a]	6	25.00[a]	25.00[a]	25.00[a]	25.00[a]	25.00[a]
T		0.1899	0.1000[b]	0.1000[b]	0.2816	0.1000[b]		0.1000[b]	0.1107	0.1000[b]	0.2330	0.1000[b]
B		25.00[a]	25.00[a]	19.78	25.00[a]	24.94		25.00[a]	25.00[a]	17.65	25.00[a]	20.47
H	2	25.00[a]	25.00[a]	25.00[a]	23.05	22.23	7	25.00[a]	25.00[a]	24.89	25.00[a]	25.00[a]
T		0.1830	0.1326	0.1000[b]	0.2103	0.1000[b]		0.1000[b]	0.1165	0.1000[b]	0.2318	0.1000[b]
B		25.00[a]	25.00[a]	20.03	25.00[a]	22.86		25.00[a]	25.00[a]	14.95	25.00[a]	23.42
H	3	25.00[a]	25.00[a]	25.00[a]	23.37	21.94	8	25.00[a]	25.00[a]	23.00	25.00[a]	25.00[a]
T		0.1869	0.1413	0.1000[a]	0.2102	0.1000[b]		0.1073	0.1244	0.1000[b]	0.2203	0.1000[b]
B		25.00[a]	25.00[a]	20.90	25.00[a]	20.51		25.00[a]	25.00[a]	14.62	25.00[a]	22.12
H	4	25.00[a]	25.00[a]	25.00[a]	25.00	25.00[a]	9	25.00[a]	25.00[a]	22.36	25.00[a]	25.00[a]
T		0.1000[b]	0.1000[b]	0.1000[b]	0.2356	0.1000[b]		0.1013	0.1319	0.1000[b]	0.2267	0.1000[b]
B		25.00[a]	25.00[a]	18.85	25.00[a]	23.70		25.00[a]	25.00[a]	19.96	25.00[a]	20.29
H	5	25.00[a]	25.00[a]	25.00[a]	25.00[a]	25.00[a]	10	25.00[a]	25.00[a]	25.00[a]	25.00[a]	25.00[a]
T		0.1025	0.1036	0.1000[b]	0.2287	0.1000[b]		0.1000[b]	0.1058	0.1000[b]	0.2296	0.1000[b]

[a]Upper bound value. [b]Lower bound value.

Table 6 Iteration histories, antenna structure, cases 11–20 (total mass, kg)

Analysis	Case 11 (2[a])	Case 12 (4[a])	Case 13 (6[a])	Case 14 (8[a])	Case 15 (10[a])	Case 16 (12[a])	Case 17 (14[a])	Case 18 (16[a])	Case 19 (18[a])	Case 20 (20[a])
1	502.14	502.14	502.14	502.14	502.14	502.14	502.14	502.14	502.14	502.14
2	485.24	482.76	462.89	420.35	470.72	475.80	474.66	474.47	466.40	434.64
3	383.18	343.98	339.86	288.81	326.51	301.89	304.10	304.66	304.00	287.18
4	302.66	276.53	260.17	229.95	247.00	228.23	230.32	231.61	226.62	224.61
5	241.31	225.43	222.33	196.72	207.82	188.16	197.86	197.41	185.11	183.32
6	216.56	200.56	202.26	180.59	185.02	175.46	178.77	178.20	174.03	172.69
7	208.12	189.41	191.17	174.55	173.76	174.21	172.28	172.25	172.93	171.31
8	206.07	187.41	186.95	172.76	171.10	173.71	171.81	171.09	172.39	169.42
9	205.78	186.31	185.45	171.64	171.25	172.95	169.76	170.49	172.02	166.81
10	204.22	185.54	183.60	170.30	170.49	171.19	171.33	170.21	171.80	166.79
11	204.19	185.21	181.66	170.41	169.99	170.91	170.02	169.72	170.04	166.22
12	204.16	185.13	181.23	170.37	169.80	170.69	169.07	169.16	169.67	165.66
13		185.09	180.70		169.64	169.68	167.59	167.78	169.37	165.61
14			178.65		169.55	169.49	166.91	167.26	169.17	166.50
15			178.06			168.38	166.23	167.00	168.92	165.30
16			177.86			167.40	166.17	166.65	167.74	165.14
17			177.31			167.01	166.01	166.29	166.91	164.95
18			176.72			166.85		165.69	165.84	164.86
19			176.67			166.76		165.46	165.64	164.80
20			176.56					165.34	165.49	
21								165.29	165.38	

[a]Number of independent control design variables.

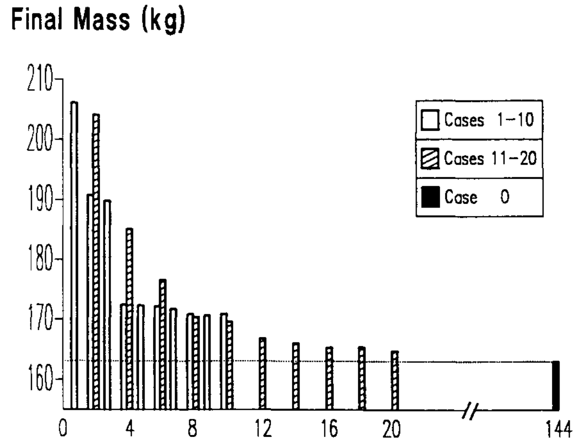

Fig. 5 Number of CDVs vs final masses, antenna structure.

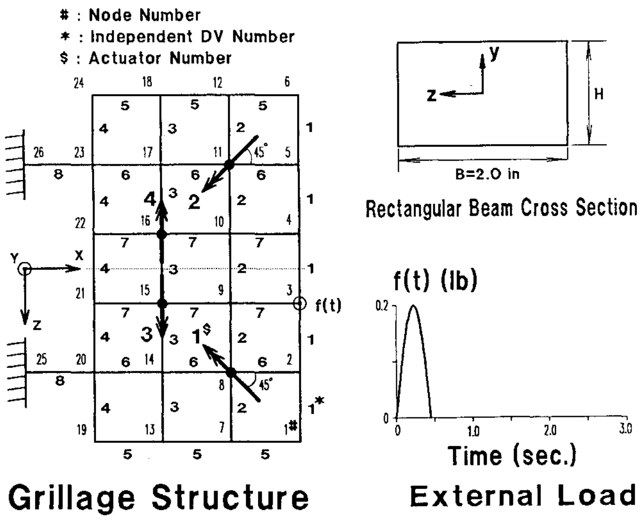

Fig. 6 Grillage structure.

Table 7 Final structural designs, antenna structure, cases 11–20 (cross sectional-dimensions, cm)

	Case	Element 1	Element 2	Elements 3, 4	Elements 5, 6	Elements 7, 8	Case	Element 1	Element 2	Elements 3, 4	Elements 5, 6	Elements 7, 8
B		25.00[a]	25.00[a]	18.99	25.00[a]	14.13		25.00[a]	25.00[a]	13.02	25.00[a]	24.32
H	11	25.00[a]	25.00[a]	25.00[a]	25.00[a]	25.00[a]	16	25.00[a]	25.00[a]	24.12	24.93	25.00[a]
T		0.1777	0.1149	0.1000[b]	0.2835	0.1000[b]		0.1000[b]	0.1341	0.1000[b]	0.2082	0.1000[b]
B		25.00[a]	25.00[a]	19.57	25.00[a]	25.00[a]		25.00[a]	25.00[a]	13.64	25.00[a]	24.70
H	12	25.00[a]	25.00[a]	25.00[a]	22.84	22.14	17	25.00[a]	25.00[a]	24.06	25.00[a]	25.00[a]
T		0.1687	0.1361	0.1000[b]	0.2032	0.1000[b]		0.1000[b]	0.1289	0.1000[b]	0.2061	0.1000[b]
B		25.00[a]	25.00[a]	13.22	25.00[a]	25.00[a]		25.00[a]	25.00[a]	15.33	25.00[a]	25.00[a]
H	13	25.00[a]	25.00[a]	25.00[a]	23.70	24.65	18	25.00[a]	25.00[a]	23.14	25.00[a]	25.00[a]
T		0.1239	0.1259	0.1000[b]	0.2271	0.1000[b]		0.1000[b]	0.1213	0.1000[b]	0.2047	0.1000[b]
B		25.00[a]	25.00[a]	22.11	25.00[a]	20.00		25.00[a]	25.00[a]	14.99	25.00[a]	24.29
H	14	25.00[a]	25.00[a]	25.00[a]	25.00[a]	25.00[a]	19	25.00[a]	25.00[a]	23.31	25.00[a]	25.00[a]
T		0.1000[b]	0.1021	0.1000[b]	0.2256	0.1000[b]		0.1000[b]	0.1186	0.1000[b]	0.2084	0.1000[b]
B		25.00[a]	25.00[a]	19.45	25.00[a]	21.32		25.00[a]	25.00[a]	14.91	25.00[a]	24.62
H	15	25.00[a]	25.00[a]	24.70	25.00[a]	25.00[a]	20	25.00[a]	25.00[a]	22.93	25.00[a]	25.00[a]
T		0.1000[b]	0.1051	0.1000[b]	0.2246	0.1000[b]		0.1000[b]	0.1205	0.1000[b]	0.2054	0.1000[b]

[a]Upper bound value. [b]Lower bound value.

Table 8 Critical constraints at the final designs, antenna structure

Case number	Final mass, kg	Critical[a] constraints Re (λ)	Im (λ)	Peak displacement	Peak control force
0	163.11	σ_{10}	ω_{d_4}	$q_{10}\ q_{16}$	$u_1\ u_2\ u_3\ u_4$
1	206.06	—	ω_{d_4}	q_{16}	u_4
2	190.70	$\sigma_8\ \sigma_9$	$\omega_{d_4}\ \omega_{d_5}$	q_{16}	u_4
3	189.81	$\sigma_4\ \sigma_8\ \sigma_9$	$\omega_{d_4}\ \omega_{d_5}$	q_{16}	u_4
4	172.46	$\sigma_3\ \sigma_4\ \sigma_8$	ω_{d_4}	q_{16}	u_4
5	172.32	$\sigma_3\ \sigma_4\ \sigma_8$	ω_{d_4}	q_{16}	u_4
6	172.17	σ_8	ω_{d_4}	q_{16}	u_4
7	171.73	σ_8	ω_{d_4}	q_{16}	$u_3\ u_4$
8	170.81	σ_8	$\omega_{d_4}\ \omega_{d_5}$	q_{16}	$u_3\ u_4$
9	170.77	$\sigma_7\ \sigma_8$	$\omega_{d_4}\ \omega_{d_5}$	q_{16}	$u_3\ u_4$
10	170.92	—	ω_{d_4}	q_{16}	$u_3\ u_4$
11	204.16	—	ω_{d_4}	q_{16}	$\dot{u}_3\ u_4$
12	185.09	$\sigma_8\ \sigma_9$	$\omega_{d_4}\ \omega_{d_5}$	q_{16}	u_4
13	176.56	$\sigma_4\ \sigma_8\ \sigma_9$	$\omega_{d_4}\ \omega_{d_5}$	q_{16}	u_4
14	170.37	σ_8	ω_{d_4}	q_{16}	u_4
15	169.55	$\sigma_4\ \sigma_8$	ω_{d_4}	q_{16}	u_4
16	166.76	$\sigma_3\ \sigma_4\ \sigma_8$	$\omega_{d_4}\ \omega_{d_5}$	q_{16}	$u_3\ u_4$
17	166.01	$\sigma_3\ \sigma_4$	$\omega_{d_4}\ \omega_{d_5}$	q_{16}	$u_3\ u_4$
18	165.29	σ_4	$\omega_{d_4}\ \omega_{d_5}$	q_{16}	$u_1\ u_3\ u_4$
19	165.38	$\sigma_4\ \sigma_7\ \sigma_8$	$\omega_{d_4}\ \omega_{d_5}$	q_{16}	$u_3\ u_4$
20	164.80	$\sigma_4\ \sigma_7$	$\omega_{d_4}\ \omega_{d_5}$	q_{16}	$u_1\ u_3\ u_4$

[a] $-0.03 \le G_j \le 0.0004$ (G_j are normalized by the allowable values).

Table 9 Initial complex eigenvalues, grillage structure $\lambda_i = \sigma_i + j\omega_{d_i}(\xi_i, \%)$

Mode number	Open loop	Closed loop
1	$-0.0001 \pm j2.29$ (0.006)	$-0.874 \pm j2.31$ (35.4)
2	$-0.001 \pm j7.05$ (0.018)	$-0.431 \pm j7.06$ (6.09)
3	$-0.007 \pm j16.4$ (0.041)	$-1.87 \pm j17.3$ (10.8)
4	$-0.009 \pm j18.6$ (0.047)	$-0.762 \pm j17.6$ (4.33)
5	$-0.018 \pm j27.1$ (0.069)	$-1.36 \pm j27.2$ (5.00)
6	$-0.039 \pm j39.5$ (0.099)	$-0.878 \pm j39.9$ (2.20)
7	$-0.040 \pm j39.9$ (0.100)	$-2.00 \pm j40.1$ (4.97)
8	$-0.062 \pm j49.7$ (0.124)	$-3.76 \pm j49.2$ (7.64)
9	$-0.091 \pm j60.2$ (0.150)	$-1.90 \pm j60.1$ (3.15)
10	$-0.119 \pm j68.9$ (0.172)	$-2.01 \pm j69.0$ (2.92)
11	$-0.135 \pm j73.6$ (0.184)	$-2.58 \pm j74.0$ (3.49)
12	$-0.146 \pm j76.5$ (0.191)	$-0.840 \pm j75.6$ (1.11)
13	$-0.231 \pm j96.0$ (0.240)	$-2.03 \pm j95.8$ (2.11)
14	$-0.267 \pm j103.0$ (0.259)	$-1.39 \pm j103.0$ (1.35)
15	$-0.281 \pm j106.0$ (0.265)	$-2.26 \pm j106.0$ (2.13)
16	$-0.316 \pm j112.0$ (0.281)	$-1.41 \pm j112.0$ (1.26)
17	$-0.353 \pm j119.0$ (0.297)	$-2.04 \pm j119.0$ (1.72)
18	$-0.413 \pm j129.0$ (0.321)	$-1.66 \pm j128.0$ (1.29)
19	$-0.505 \pm j142.0$ (0.355)	$-2.81 \pm j142.0$ (1.98)
20	$-0.524 \pm j145.0$ (0.362)	$-1.65 \pm j145.0$ (1.14)

Table 10 Independent control design variables (CDV), grillage structure

	Case 1	Case 2	Case 3	Case 4	Case 5	Case 6
CDV	$\alpha_1 = \cdots = \alpha_{25}$	$\alpha_1, \alpha_2 = \cdots = \alpha_{25}$	$\alpha_1, \alpha_2,$ $\alpha_3 = \cdots = \alpha_{25}$	$\alpha_1, \cdots, \alpha_4,$ $\alpha_5 = \cdots = \alpha_{25}$	$\alpha_1, \cdots, \alpha_9,$ $\alpha_{10} = \cdots = \alpha_{25}$	$\alpha_1, \cdots, \alpha_{19},$ $\alpha_{20} = \cdots = \alpha_{25}$
Number of independent CDVs	1	2	3	5	10	20

Table 11 Final structural design variables, grillage structure (depth, cm)

Design variable number	1	2	3	4	5	6	7	8
Case 1	0.2849	0.1698	0.1000[a]	0.1953	0.1502	0.3656	0.2299	0.4724
Case 2	0.2768	0.1806	0.1000[a]	0.1973	0.1479	0.3626	0.2180	0.5021
Case 3	0.2510	0.1936	0.1000[a]	0.1769	0.1429	0.3670	0.2221	0.4951
Case 4	0.2392	0.1985	0.1000[a]	0.1788	0.1373	0.3691	0.2222	0.4719
Case 5	0.2557	0.1191	0.1000[a]	0.1908	0.1000[a]	0.3701	0.1622	0.5880
Case 6	0.2466	0.1125	0.1000[a]	0.1560	0.1000[a]	0.4128	0.1137	0.5573

[a]Lower bound value.

Table 12 Iteration histories, grillage structure, cases 1-6 total mass (lb · s²/in.)

Analysis	Case 1 (1[a])	Case 2 (2[a])	Case 3 (3[a])	Case 4 (5[a])	Case 5 (10[a])	Case 6 (20[a])
1	0.1294	0.1294	0.1294	0.1294	0.1294	0.1294
2	0.1448	0.1433	0.1440	0.1442	0.1442	0.1468
3	0.1332	0.1327	0.1369	0.1353	0.1352	0.1366
4	0.1272	0.1295	0.1317	0.1258	0.1261	0.1298
5	0.1231	0.1256	0.1238	0.1222	0.1257	0.1223
6	0.1211	0.1247	0.1206	0.1212	0.1215	0.1168
7	0.1211	0.1200	0.1185	0.1197	0.1182	0.1163
8	0.1198	0.1189	0.1172	0.1178	0.1170	0.1139
9	0.1192	0.1189	0.1166	0.1170	0.1145	0.1114
10	0.1192	0.1188	0.1172	0.1174	0.1136	0.1103
11	0.1194		0.1173	0.1173	0.1126	0.1103
12	0.1191		0.1172	0.1171	0.1111	0.1089
13	0.1191		0.1177	0.1162	0.1107	0.1088
14			0.1173	0.1162	0.1111	0.1080
15			0.1168	0.1162	0.1099	0.1065
16			0.1170	0.1159	0.1098	0.1053
17			0.1169	0.1158	0.1098	0.1047
18			0.1169	0.1159	0.1093	0.1044
19				0.1160	0.1091	0.1039
20				0.1158	0.1091	0.1036
21				0.1157	0.1093	0.1042
22				0.1157	0.1083	0.1041
23					0.1080	0.1040
24					0.1082	0.1039
25					0.1083	
26					0.1082	
27					0.1083	

[a]Number of independent control design variables.

the directions shown in Fig. 6. The mass of each actuator (1.296×10^{-3} lb · s²/in.) is modeled as a fixed nonstructural mass. Initial control gains are obtained by solving 25 sets of 2×2 decoupled Riccati equations with diagonal control weighting matrices $[R_i] = 1/200$ diag[2, 2, 1, 1] and diagonal 2×2 state weighting matrices $[Q_i] = \text{diag}(\omega_i^2, 1)$, $i = 1, \ldots, 25$ [see Eq. (15)]. Initial open-loop and closed-loop eigenvalues are given in Table 9. Transient responses are considered for a time period $0 \le t \le 3$ s, and the lowest 40 out of 144 complex modes are used.

The total mass is minimized subject to a transient loading at node 3 in the Y direction, which is a half-sine pulse of magnitude 0.2 lb and frequency 7 rad/s. Structural design variable linking is used to impose symmetry with respect to the XY plane on the structure and as a result there are eight independent structural design variables (see Fig. 6). Lower and upper

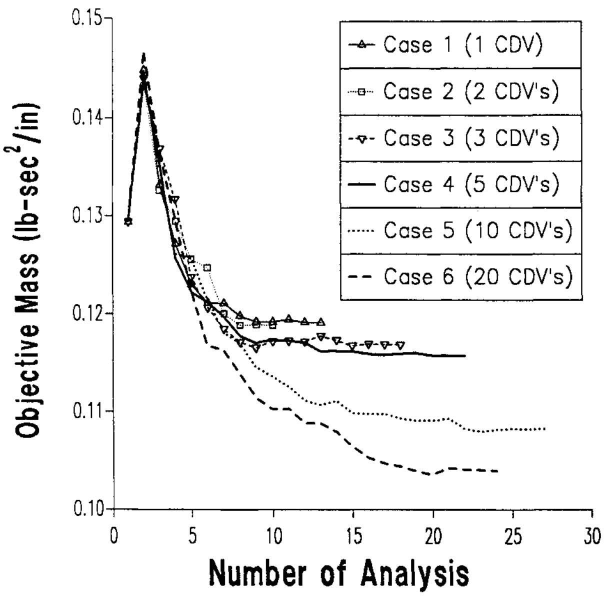

Fig. 7 Grillage structure iteration histories, cases 1-6.

limits on the member depths are 0.1 and 1.0 in., respectively. In this example behavior constraints are imposed on 1) the modal damping factors of the first 20 modes ($\xi_i \ge 1\%$, $i = 1, \ldots, 20$); 2) the transient displacements at nodes 1-6, 7, 13, 19, 12, 18, and 24 in the Y direction [i.e., $q(t) \le 0.2$ in.]; and 3) the transient control torques of all actuators [$u(t) \le 2.5$ lb · in.].

At the initial structural and control design, all of the damping ratio and control force constraints are satisfied, but transient displacement constraints are infeasible by as much as 68%. Hybrid approximation in terms of depths of the members and linear approximation in terms of the control design variables are used to generate approximate optimization problems.

In this example, the number of elements in the feedback gain matrix is very large ($M \times 2N = 4 \times 2 \cdot 72 = 576$), so that it is almost impossible to use all of the gain elements directly as independent design variables. Six cases are investigated that are similar to cases 1–10 of the preceding example, namely, the participation coefficients α_i of $[H^o]^{(i)}$ [see Eq. (26)] are control system design variables. These α_i are further linked so that in each case the number of independent control design variables is different (see Table 10).

Final member depths are given in Table 11. In all cases the depth of member 3 (node 13–18) has its lower bound value,

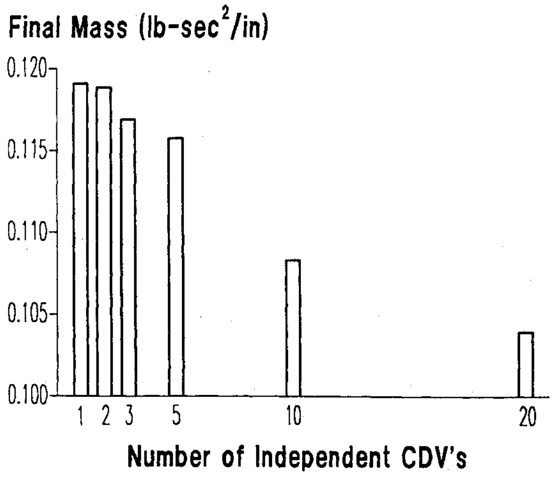

Fig. 8 Number of CDVs vs final masses, grillage structure.

and in cases 5 and 6 depths of members 5 (node 1–19) and 10 (node 6–24) also have lower bound values in addition to member 3. Iteration histories are given in Table 12 and also shown graphically in Fig. 7. In Fig. 8 final mass values of the six cases are compared with the number of independent control design variables. Similar observations as in the first example can be made, namely, as the number of independent control design variables is increased from 1 to 20, the final objective mass value decreases (from 0.1191 to 0.1039, a 12.8% reduction), but the total number of analyses required for the convergence tends to increase. The final closed-loop complex eigenvalues and modal damping factors are given in Table 13.

In all of the cases transient displacement constraints at node 1 and transient control force constraints on actuators 3 and 4 are active at the final design in addition to the critical damping ratio constraints (see Table 13).

VII. Conclusion

It is shown that the design variable linking concept can be extended to control system design variables. In the context of

Table 13 Final closed-loop eigenvalues, grillage structure
$\lambda_i = \sigma_i + j\omega_{d_i}$ (ξ_i, %)

Mode number	Case 1	Case 2	Case 3	Case 4	Case 5	Case 6
1	−1.58 ± j4.85 (30.9)	−1.62 ± j5.03 (30.7)	−1.89 ± j5.14 (34.4)	−2.08 ± j5.19 (37.1)	−2.22 ± j5.92 (35.1)	−1.85 ± j6.56 (27.1)
2	−0.438 ± j9.76 (4.49)	−0.321 ± j9.93 (3.23)	−0.103 ± j9.90 (1.04)	−0.998E−01 ± j9.76 (1.02[a])	−0.115 ± j10.5 (1.09)	−0.112 ± j10.7 (1.05)
3	−2.26 ± j20.4 (11.0)	−1.75 ± j20.4 (8.53)	−2.36 ± j20.0 (11.7)	−10.4 ± j19.9 (46.2)	−1.16 ± j22.2 (5.21)	−0.209 ± j20.3 (1.03[a])
4	−1.53 ± j24.7 (6.17)	−1.08 ± j25.4 (4.25)	−2.10 ± j24.7 (8.50)	−1.44 ± j22.0 (6.55)	−4.02 ± j22.6 (17.5)	−6.55 ± j22.2 (28.3)
5	−2.53 ± j30.5 (8.26)	−2.08 ± j31.0 (6.70)	−2.58 ± j29.9 (8.58)	−2.71 ± j30.0 (9.01)	−1.92 ± j28.6 (6.70)	−0.724 ± j26.2 (2.77)
6	−0.415 ± j38.9 (1.06)	−0.404 ± j39.6 (1.02[a])	−0.423 ± j38.7 (1.09)	−0.384 ± j38.1 (1.01[a])	−0.397 ± j37.0 (1.07)	−11.4 ± j35.1 (30.9)
7	−2.24 ± j40.1 (5.59)	−1.96 ± j39.9 (4.91)	−2.62 ± j39.2 (6.66)	−2.01 ± j38.8 (5.19)	−1.27 ± j38.6 (3.30)	−0.605 ± j35.4 (1.71)
8	−1.36 ± j50.7 (2.68)	−1.87 ± j51.5 (3.63)	−15.5 ± j47.9 (30.7)	−13.7 ± j48.3 (27.2)	−12.0 ± j45.8 (25.4)	−0.397 ± j37.3 (1.07)
9	−15.4 ± j51.7 (28.6)	−10.9 ± j53.2 (20.1)	−2.44 ± j51.2 (4.75)	−2.24 ± j50.5 (4.42)	−0.534 ± j48.3 (1.10)	−0.666 ± j44.3 (1.50)
10	−2.49 ± j55.1 (4.51)	−1.98 ± j54.9 (3.60)	−3.14 ± j52.3 (5.99)	−3.07 ± j51.7 (5.92)	−0.615 ± j48.7 (1.26)	−0.479 ± j47.9 (1.00[a])
11	−1.14 ± j62.4 (1.83)	−0.674 ± j63.6 (1.06)	−0.995 ± j62.3 (1.60)	−0.627 ± j61.8 (1.02[a])	−0.525 ± j52.2 (1.00[a])	−0.496 ± j48.4 (1.02[a])
12	−0.634 ± j63.3 (1.00[a])	−0.638 ± j63.9 (1.00[a])	−0.625 ± j62.3 (1.00[a])	−0.948 ± j62.7 (1.51)	−0.648 ± j56.1 (1.15)	−0.539 ± j52.8 (1.02[a])
13	−3.38 ± j74.1 (4.55)	−2.56 ± j75.0 (3.40)	−2.54 ± j74.0 (3.42)	−2.23 ± j72.7 (3.06)	−3.55 ± j65.0 (5.45)	−1.93 ± j54.6 (3.54)
14	−0.944 ± j93.1 (1.01[a])	−0.934 ± j91.7 (1.02[a])	−0.975 ± j88.5 (1.10)	−0.881 ± j86.6 (1.02[a])	−0.749 ± j72.7 (1.03[a])	−3.35 ± j66.1 (5.06)
15	−17.5 ± j97.6 (17.7)	−11.8 ± j100.0 (11.7)	−20.7 ± j95.4 (21.2)	−19.4 ± j96.7 (19.7)	−2.08 ± j77.5 (2.68)	−37.0 ± j66.3 (48.8)
16	−2.26 ± j104.0 (2.16)	−2.88 ± j101.0 (2.85)	−3.96 ± j99.3 (3.99)	−2.12 ± j97.2 (2.19)	−2.63 ± j79.0 (3.32)	−0.742 ± j71.9 (1.03[a])
17	−3.28 ± j105.0 (3.12)	−4.61 ± j105.0 (4.40)	−2.13 ± j99.9 (2.13)	−3.81 ± j98.4 (3.87)	−12.6 ± j85.6 (14.5)	−7.59 ± j75.7 (9.97)
18	−2.67 ± j106.0 (2.51)	−1.08 ± j105.0 (1.03[a])	−1.04 ± j101.0 (1.03[a])	−0.986 ± j98.7 (1.00[a])	−1.62 ± j99.0 (1.63)	−1.04 ± j90.5 (1.15)
19	−1.21 ± j120.0 (1.01[a])	−1.24 ± j121.0 (1.03[a])	−1.20 ± j119.0 (1.01[a])	−1.19 ± j117.0 (1.01[a])	−2.36 ± j110.0 (2.15)	−1.35 ± j95.1 (1.42)
20	−1.43 ± j142.0 (1.01[a])	−1.49 ± j140.0 (1.06)	−1.36 ± j135.0 (1.00[a])	−1.40 ± j135.0 (1.04)	−1.33 ± j133.0 (1.00[a])	−1.34 ± j131. (1.02[a])

[a]Critical damping ratio constraints ($0.999 \le \xi_i \le 1.03$).

full-state feedback control, design variable linking makes it possible to treat structural design variables and control design variables simultaneously without having to deal with prohibitively large numbers of design variables (see example 2, which has 576 possible control variables).

A new block-type control design variable linking scheme based on representing the feedback gain matrix $[H]$ (or $[H_p]$ and $[H_v]$) as the linear combination of r "basis matrices" corresponding to different modes is introduced. This linking scheme is based on calculation of the initial feedback gain matrix by solving r sets of 2×2 Riccati equations. The solution of each 2×2 Riccati equation depends on the corresponding modal information and contributes a component matrix $[H^o]^{(i)}$ (or $[H_p^o]^{(i)}$ and $[H_v^o]$) to the initial gain matrix. Each component matrix obtained is treated as a basis in this control design variable linking scheme, and the actual feedback gain matrix is then expressed as a linear combination of these basis matrices, i.e.,

$$[H] = \sum_{i=1}^{r} \alpha_i [H^o]^{(i)}$$

or

$$[H] = \sum_{i=1}^{r} \left[\alpha_i [H_p^o]^{(i)} \, \alpha_{i+r} [H_v^o]^{(i)} \right]$$

During optimization the participation coefficients (α_i) of the basis matrices are treated as independent design variables along with the cross-sectional dimensions of the structural elements.

Numerical results for various example problems show that the new linking scheme is superior to previously reported control design variable linking arrangements, based on various column-wise and row-wise linking strategies (see example 1). The new linking scheme improves performance in the sense that for any fixed number of independent control design variables it leads to designs with significantly lower mass than those achieved by using the row and column linking schemes reported in Ref. 12.

Acknowledgment

The sponsorship provided by the NASA Langley Research Center under NASA Grant NSG 1490 is gratefully acknowledged.

References

[1]Nurre, G. S., Ryan, R. S., Scofield, H. N., and Sims, J. L., "Dynamics and Control of Large Space Structures," *Journal of Guidance, Control, and Dynamics,* Vol. 7, No. 5, 1984, pp. 514–526.

[2]Haftka, R. T., Martinovic, Z. N., and Hallauer, W. L., "Enhanced Vibration Controllability by Minor Structural Modification," *AIAA Journal,* Vol. 23, No. 8, 1985, pp. 1260–1266.

[3]Khot, N. S., Venkayya, V. B., and Eastep, F. E., "Optimal Structural Modifications to Enhance the Active Vibration Control of Flexible Structures," *AIAA Journal,* Vol. 24, No. 8, 1986, pp. 1368–1374.

[4]Lust, R. V., and Schmit, L. A., "Control Augmented Structural Synthesis," NASA CR-4132, April 1988.

[5]Thomas, H. L., Sepulveda, A. E., and Schmit, L. A., "Improved Approximations for Control Augmented Structural Synthesis," *AIAA Journal,* Vol. 30, No. 1, 1992, pp. 171–179.

[6]Junkins, J. L., and Rew, D. W., "Unified Optimization of Structures and Controllers," *Large Space Structures: Dynamics and Control,* edited by S. N. Atluri and A. K. Amos, Springer-Verlag, Berlin, 1988, pp. 323–353.

[7]McLaren, M. D., and Slater, G. L., "A Covariance Approach to Integrated Control/Structure Optimization," *AIAA Dynamics Specialist Conference* (Long Beach, CA), AIAA, Washington, DC, 1990, pp. 189–205; see also AIAA Paper 90-1211.

[8]Sepulveda, A. E., and Schmit, L. A., "Optimal Placement of Actuators and Sensors in Control-Augmented Structural Optimization," *International Journal for Numerical Methods in Engineering,* Vol. 32, No. 6, 1991, pp. 1165–1187.

[9]Salama, M., Garba, J., Demestz, L., and Udwadia, F., "Simultaneous Optimization of Controlled Structures," *Computational Mechanics,* Vol. 3, 1988, pp. 275–282.

[10]Miller, D. F., and Shim, J., "Gradient-Based Combined Structural and Control Optimization," *Journal of Guidance, Control, and Dynamics,* Vol. 10, No. 3, 1987, pp. 291–298.

[11]Grandhi, R. V., "Structural and Control Optimization of Space Structures," *Computers and Structures,* Vol. 31, No. 2, 1989, pp. 139–150.

[12]Jin, I. M., and Schmit, L. A., "Control Design Variable Linking for Optimization of Structural/Control Systems," *AIAA Journal,* Vol. 30, No. 7, 1992, pp. 1892–1900.

[13]Jin, I. M., "Control Design Variable Linking for Optimization of Structural/Control Systems," Ph.D. Dissertation, Univ. of California, Los Angeles, CA, 1991.

[14]Schmit, L. A., and Farshi, B., "Some Approximation Concepts for Efficient Structural Synthesis," *AIAA Journal,* Vol. 12, No. 5, 1974, pp. 692–699.

[15]Schmit, L. A., and Miura, H., "Approximation Concepts for Efficient Structural Synthesis," NASA CR-2552, March 1976.

[16]Starnes, J. R., and Haftka, R. T., "Preliminary Design of Composite Wings for Buckling, Stress and Displacement Constraints," *Journal of Aircraft,* Vol. 16, No. 8, 1979, pp. 564–570.

[17]Haftka, R. T., and Gürdal, Z., *Elements of Structural Optimization,* 3rd ed., Kluwer, Boston, 1992.

[18]Vanderplaats, G. N., "CONMIN—A Fortran Program for Constrained Function Minimization," NASA TM-X-62,682, Aug. 1973.